International Journal of Mass Spectrometry 273 (2008) 95–104

Contents lists available at ScienceDirect

International Journal of Mass Spectrometry

journal homepage: www.elsevier.com/locate/ijms

Multi-component elemental and molecular analysis of lanthanides by capillary electrophoresis–electrospray mass spectrometry (CE–ESI-MS)

Aurélien Pitois [1], Laura Aldave de Las Heras, Maria Betti *

European Commission, Joint Research Centre, Institute for Transuranium Elements, P.O. Box 2340, D-76125 Karlsruhe, Germany

ARTICLE INFO

Article history:
Received 29 January 2008
Received in revised form 13 March 2008
Accepted 14 March 2008
Available online 29 March 2008

Keywords:
Capillary electrophoresis
Electrospray mass spectrometry
Lanthanide
Complexation
Structural information

ABSTRACT

Electrospray mass spectrometry is a method of choice for individual elemental and molecular analysis of uncomplexed or complexed metal ions in solution. The multi-component elemental and molecular analysis of lanthanides is however hindered by the existence of isobaric interferences, therefore a previous chemical separation is required before mass spectrometric analysis. The whole lanthanide series has been separated by capillary electrophoresis using partial complexation and detected by electrospray mass spectrometry. The multi-component capability of coupled capillary electrophoresis–electrospray mass spectrometry for elemental and molecular analysis has been shown by adjusting the degree of declustering and molecular fragmentation in the mass spectrometer interface region. Three different modes have been defined as a function of the fragmentation potential applied (high, low and intermediate fragmentation potentials). For a high fragmentation potential, the system operates as an elemental detector: spectra representing mainly singly charged lanthanide oxide or lanthanide metal ion are observed. These spectra can be related to the dissociation energies of the lanthanide oxide bond and to the lanthanide electronic properties. For a low fragmentation potential, the system operates as a molecular detector: structural information on the mixed complexes formed in the capillary during the electrophoretic separation are obtained. The intermediate fragmentation potentials enable the study of the different steps of declustering.

1. Introduction

Lanthanides, because of their interesting physical and chemical properties, have been widely used in diverse scientific and technological fields such as metallurgy, material science, microelectronics or medical diagnostics [1]. As a result of their increasing applications, more information on their chemical behaviour in a multi-component system are necessary in order to carry out an accurate and precise determination of them in different matrices. Atomic-based elemental analysis techniques such as atomic absorption spectroscopy (AAS) [2], inductively coupled plasma-atomic emission spectroscopy (ICP-AES) [3,4] and inductively coupled plasma-mass spectrometry (ICP-MS) [5–8] have been largely used for the determination of lanthanides in water [9], and in geological [10–15], and environmental materials [16]. These element specific systems present the advantage of a high selectivity and sensitivity, and quantification of lanthanides at trace level (pg/mL to mg/mL concentration range) has been achieved for these materials. No information on oxidation state, molecular forms and complexation is nevertheless obtained with these systems. These information are however of great interest for a better understanding of the lanthanide behaviour in different environments. For example, in aquatic environments, the fate and transport, i.e., both mobilisation and retardation, of lanthanides are strongly correlated to the presence of complexing agents in solution. Elemental detection systems have to be complemented by molecular detection systems. Electrospray mass spectrometry (ESI-MS), as a soft molecular detection technique, is a method of choice for elemental and structural information, since the degree of declustering and molecular fragmentation in the mass spectrometer interface region can be adjusted. Three different modes have been determined by Agnes and Horlick as a function of the fragmentation potential applied (high, low and intermediate fragmentation potentials) [17]. When high interface voltages are applied, the ion is declustered to the oxide ion or to the bare metal ion. This is the mode for elemental analysis. When low interface voltages are applied, the ion-solvent cluster distribution generated during the electrospray process is preserved relatively intact. This is the mode for molecular analysis. Partial declustering occurs for intermediate fragmentation potentials.

Electrospray mass spectrometry has been first applied to the analysis of uncomplexed metal ions and organometallic species in various solution media. The elemental analysis of alkali metals (Li,

* Corresponding author.
E-mail address: maria.betti@ec.europa.eu (M. Betti).
[1] Present address: European Commission, Joint Research Centre, Institute for Energy, P.O. Box 2, NL-1755 ZG Petten, The Netherlands.

1387-3806/$ – see front matter © 2008 Elsevier B.V. All rights reserved.
doi:10.1016/j.ijms.2008.03.010

Na, K, Rb and Cs) and transition metals (Cr, Mn, Fe, Co, Ni, Cu, Zn, Ag and Cd) has been performed in aqueous and methanolic media [18]. The elemental analysis of uncomplexed lanthanides has been also studied in solution [19]. The solvation of metal ions in solution has been observed for the first time by ESI-MS [20,21]. Two transition metals (Co and Mn) have been investigated at different fragmentation potentials and the three modes have been defined [17]. Electrospray mass spectrometry has been also applied to the analysis of complexed metal ions in solution. The complexation of nickel with EDTA has been studied [22]. Information on metal–ligand interactions for actinides [23,24] and fission products speciation [25–29] has been also obtained. All these studies have highlighted the potential of ESI-MS for elemental and molecular analysis. However, most of these studies were monocomponent: each element was studied individually. Multi-component analysis is very often hindered by interferences from isobaric atomic ions, polyatomic ions or molecular ions. When determining lanthanides interferences are numerous. When elemental analysis is performed, lanthanide isobars can interfere each other as well as the formation of oxide can give place to overlapping at certain masses. When molecular analysis is performed, interferences are even more numerous since a quite complex ion-solvent cluster distribution generated during the electrospray process is observed for each element. To overcome these interferences, a previous chemical separation of interfering elements is required before mass spectrometric analysis. The hyphenation of a separation technique such as ionic chromatography or capillary electrophoresis with an ESI-MS has been already applied to the analysis of a mixture of metal ions [30,31]. These hyphenations facilitated multi-elemental analyses and reduced considerably the complexity of the mass spectra. Ionic chromatography and capillary electrophoresis have been already coupled with an ICP-MS for the quantification of the whole lanthanide series at ultratrace level and detection limits in the ng/mL and pg/mL ranges have been achieved by IC-ICP-MS and CE–ICP-MS, respectively [32–34]. Compared to chromatographic techniques, the use of capillary electrophoresis for the separation offers advantages in terms of low sample volume, simplicity, reduced time and cost of analysis.

In this study, the whole lanthanide series has been separated by capillary electrophoresis using partial complexation with picolinic acid and HIBA and detected by electrospray mass spectrometry. Electrospray parameters such as make-up liquid flow rate and composition have been optimised to obtain a stable and efficient electrospray process and to keep a good separation of the whole lanthanide series. The three ESI-MS modes (high, low and intermediate fragmentation potentials) have been studied in details. The possibility to exploit ESI-MS as an elemental and molecular detector has been investigated and is here discussed.

2. Experimental

2.1. Instrumentation

The instrumental set-up consisted of an Agilent 3D capillary electrophoresis (Agilent Technologies Deutschland GmbH, Waldbronn, Germany) coupled with an Agilent 1100 Series LC/MSD SL electrospray mass spectrometer (Agilent Technologies Deutschland GmbH, Waldbronn, Germany) as a detector.

The experimental conditions for the capillary electrophoresis, the interface and the ESI-MS are summarised in Table 1.

Table 1
Experimental conditions for the capillary electrophoresis, the interface and the ESI-MS

Capillary electrophoresis	Agilent 3D capillary electrophoresis
Capillary	Fused silica, 120 cm length, 50 μm i.d.
Buffer	0.8 mM picolinic acid, 10 mM HIBA, 25 mM formic acid, pH 4.7 adjusted by TRIS
Temperature	20 °C
Voltage	28 kV (field strength: 23.3 kV m^{-1})
Injection	Hydrodynamic mode, 5 s, 50 mbar, 38 nL
Interface CE–ESI-MS	Agilent 1100 Series LC/MSD SL
Make-up liquid flow rate	4 μL/min, isocratic pump
Make-up liquid composition	5 mM ammonium acetate in methanol
ESI-MS	Agilent 1100 Series LC/MSD SL
ESI-MS capillary voltage	−5.6 kV
Nebulising, drying and curtain gas	Nitrogen N_2
Gas flow rate	10 L/min
Nebuliser pressure	10 psig
Drying gas temperature	300 °C
Fragmentation potential	From 40 V to 390 V
High fragmentation potentials	>340 V
Low fragmentation potentials	<100 V
Intermediate fragmentation potentials	160 V, 190 V and 220 V
Scan type	Positive ion mode
Scan speed	1.3 s/scan
Scan range	According to the fragmentation potential

2.2. Chemicals

Lanthanide standards (La, Ce, Pr, Nd, Sm, Eu, Gd, Tb, Dy, Ho, Er, Tm, Yb, Lu) were provided by SPEX CertiPrep (Metuchen, NJ, USA) as 1000 μg/mL stock standard solutions. Picolinic acid (2-pyridinecarboxylic acid) and TRIS (Tris[hydroxymethyl]aminomethane) were obtained from Sigma–Aldrich (Steinheim, Germany), ammonium acetate and formic acid from Merck (Darmstadt, Germany) and HIBA (α-hydroxyisobutyric acid) from Fluka (Buchs, Switzerland). Other chemicals such as methanol, ammonia and nitric acid were analytical-reagent grade from Merck (Darmstadt, Germany). Water purified in a Milli-Q system (Millipore, Eschborn, Germany) was used throughout the procedure. All standard solutions and samples were prepared by dilution in mass in polyethylene bottles previously cleaned according to a procedure for trace element analysis. A CE buffer containing 0.8 mM picolinic acid, 10 mM HIBA and 25 mM formic acid at pH 4.7 adjusted by TRIS [35] and a make-up liquid composed of 5 mM ammonium acetate in methanol were employed for the determination of lanthanides. The fused-silica capillaries were provided by Polymicro Technologies (Polymicro Technologies, Phoenix, AZ, USA). The capillary was flushed with running buffer for 15 min at the beginning of each day. A washing step of 5 min with running buffer was applied between each run. The capillary was also flushed with 1 M NaOH, Milli-Q water and air consecutively each for a 10 min duration at the end of each day. All system control, data acquisition and data evaluation were performed with G2201AA Agilent ChemStation software.

3. Results and discussion

3.1. Optimisation of the electrospray parameters

Electrospray parameters such as make-up liquid flow rate and composition have been optimised. Particular attention has been paid to the stability and efficiency of the electrospray process as well as to the non-alteration of the sample properties by the electrospray process.

3.2. Optimisation of the make-up liquid flow rate

Make-up liquid flow rates ranging from 2 μL/min to 6 μL/min have been studied. Methanol, a very volatile solvent, has been first chosen as a make-up liquid to avoid any problem of volatility dur-

ing the electrospray process. Unstable MS signals are obtained for flow rates lower than 3 μL/min. A stable MS signal is observed for a 4 μL/min flow rate and the transfer of ions from the liquid phase to the gas phase results to be efficient, since high signal sensitivity is achieved. Stable MS signals are also observed for flow rates higher than 4 μL/min. However, optimal sensitivity is obviously achieved by delivering reduced flow rates, since the CE liquid outlet is less diluted.

3.3. Optimisation of the make-up liquid composition

Various methanol/water ratios (1/1 (v/v), 3/1 (v/v) and methanol only) have been studied. As methanol is more volatile than water, the relative volatility of the make-up liquid is increasing with the methanol volume used. Unstable MS signal and low sensitivity are observed for a 1/1 (v/v) methanol/water ratio. Stable MS signals and high sensitivity are obtained with increasing make-up liquid volatility, since the droplets formed at the end of the sprayer are more easily evaporated and ionised. However, for all these different make-up liquid compositions, the peak corresponding to the cerium is never observed. Only thirteen lanthanides appear on the CE–ESI-MS electropherogram using a CE buffer composed of 0.8 mM picolinic acid, 10 mM HIBA and 25 mM formic acid at pH 4.7 and a make-up liquid composed of a methanol–water mixture (Fig. 1).

All 14 lanthanides have been nevertheless detected in these conditions by direct UV absorption spectrophotometry [35]. As a result, a phenomenon preventing the cerium to be detected by ESI-MS probably occurs during the electrospray process. The physico-chemical properties of cerium, in particular its $E_{4/3}$ redox potential, may explain this phenomenon. Indeed, contrary to the other lanthanides, which have an $E_{4/3}$ redox potential higher than 3.1 V, cerium has a lower $E_{4/3}$ redox potential equal to 1.74 V [28]. As a result, cerium can exhibit relatively easily the oxidation state +IV. It is in fact well known that, although the lanthanides exhibit a marked trivalent oxidation state, the tetravalent ions Ce^{4+} may exist in aqueous solutions as a consequence of small energy difference between the 4f and 5d electrons of this element [28]. It has been also shown that the ESI source can be considered as a controlled-current electrolytic cell and consequently redox reactions (especially at the end of the sprayer) may produce ions with an oxidation state different from that present in solution [36]. Thus, it seems possible that a redox reaction occurs at the end of the sprayer and that cerium ions are oxidised from the oxidation state +III to the oxidation state +IV during the electrospray process in these experimental conditions. It has been also observed experimentally that a much higher sensitivity is obtained for the ions presenting the oxidation state +III compared to the ions presenting the oxidation state +IV.

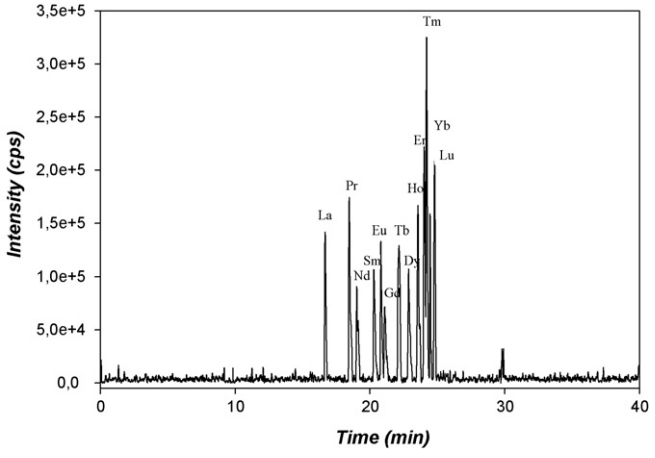

Fig. 1. Electropherogram of the separation of lanthanides by CE–ESI-MS. In these experimental conditions the cerium peak is not present in the spectrum. Charge and mass number of ions measured: $^{139}La^+$, $^{141}Pr^+$, $^{142, 143, 144, 145, 146, 148, 150}Nd^+$, $^{144, 147, 148, 149, 150, 152, 154}Sm^+$, $^{151, 153}Eu^+$, $^{154, 155, 156, 157, 158, 160}Gd^+$, $^{159}Tb^+$, $^{160, 161, 162, 163, 164}Dy^+$, $^{165}Ho^+$, $^{164, 166, 167, 168, 170}Er^+$, $^{169}Tm^+$, $^{170, 171, 172, 173, 174, 176}Yb^+$, $^{175, 176}Lu^+$. Separation buffer: 0.8 mM picolinic acid, 10 mM HIBA, 25 mM formic acid at pH 4.7; make-up liquid: methanol–water mixtures.

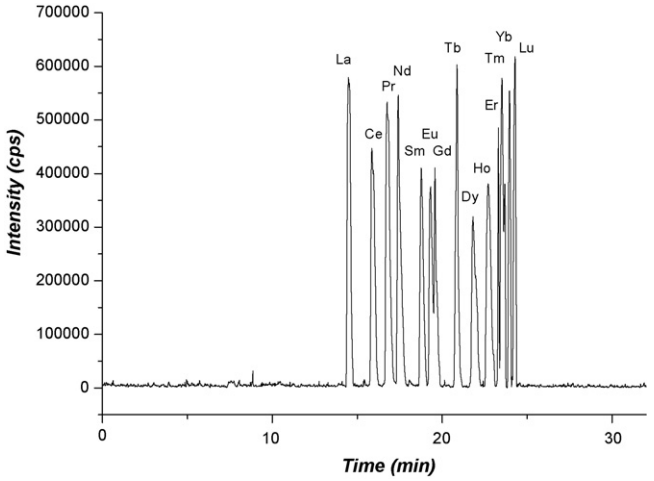

Fig. 2. Electropherogram of the separation of the 14 lanthanides by CE–ESI-MS in experimental conditions stabilising the oxidation state (+III) of Ce that appears in the spectrum. Charge and mass number of ions measured: $^{139}La^+$, $^{140, 142}Ce^+$, $^{141}Pr^+$, $^{142, 143, 144, 145, 146, 148, 150}Nd^+$, $^{144, 147, 148, 149, 150, 152, 154}Sm^+$, $^{151, 153}Eu^+$, $^{154, 155, 156, 157, 158, 160}Gd^+$, $^{159}Tb^+$, $^{160, 161, 162, 163, 164}Dy^+$, $^{165}Ho^+$, $^{164, 166, 167, 168, 170}Er^+$, $^{169}Tm^+$, $^{170, 171, 172, 173, 174, 176}Yb^+$, $^{175, 176}Lu^+$. Separation buffer: 0.8 mM picolinic acid, 10 mM HIBA, 25 mM formic acid at pH 4.7; make-up liquid: methanol and 5 mM ammonium acetate.

The make-up liquid composition has been modified to prevent redox modifications during the electrospray process. The addition of an external electrolyte such as ammonium acetate, a commonly used volatile ESI stabiliser, to the make-up liquid is known to improve the electrospray process [37]. 5 mM ammonium acetate has been added to each methanol/water ratio previously investigated and its influence on the electrospray process has been assessed. Stable MS signal and good sensitivity are obtained for a 1/1 (v/v), respectively 3/1 (v/v), methanol/water ratio 5 mM ammonium acetate make-up liquid and a 4 μL/min flow rate, showing that ammonium acetate acts effectively as an ESI stabiliser. However, still no peak corresponding to the cerium appears on the electropherogram. The peak corresponding to the cerium appears only when a methanol only 5 mM ammonium acetate make-up liquid is used. The complete separation of all fourteen lanthanides by CE–ESI-MS is shown in Fig. 2. Good repeatability in terms of migration times and peak areas have been found: the apparent mobility values μ for each lanthanide are in good agreement with those found by CE–ICP-MS [33] and intra- and inter-day peak area repeatabilities of 3% and 5%, respectively have been obtained.

3.4. The three modes of ESI-MS: high, low and intermediate fragmentation potentials

The modes corresponding to high and low fragmentation potentials will be presented for the whole lanthanide series. The intermediary mode will be shown more in detail with an example: the element terbium.

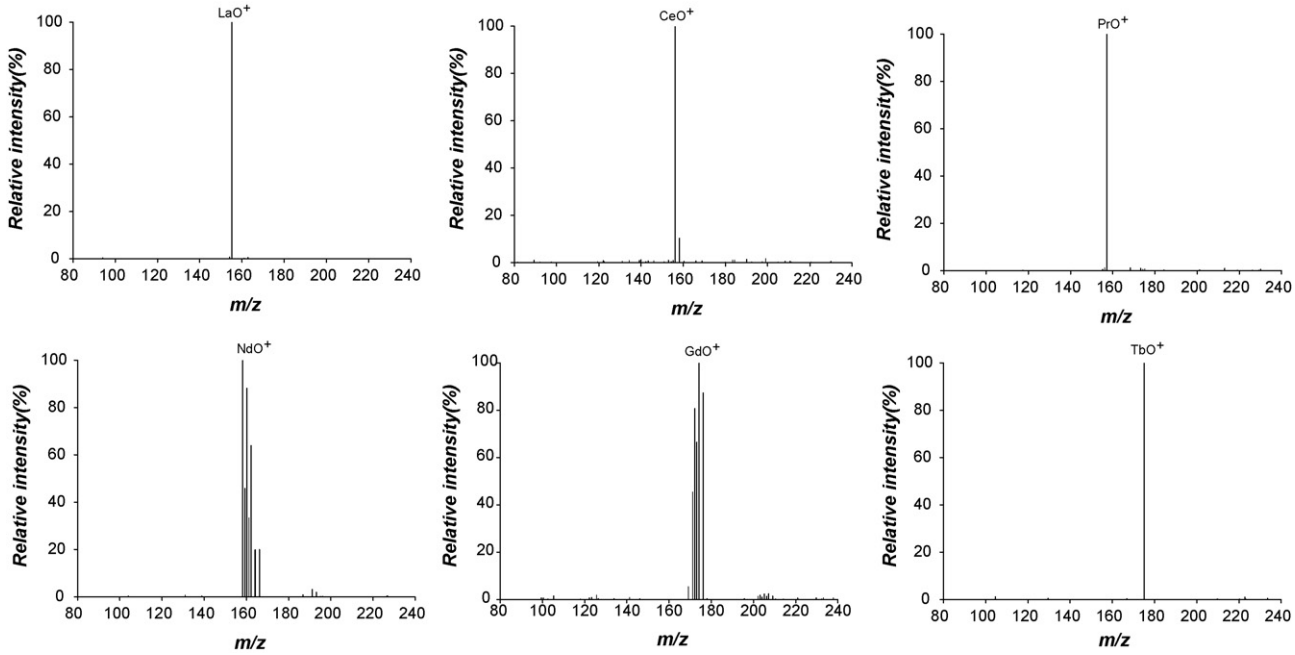

Fig. 3. ESI-MS spectra of the lanthanides, which present the ion LnO^+ as a unique form at high fragmentation potentials.

3.5. High fragmentation potential

When high fragmentation potentials are applied at the interface (fragmentation potentials higher than 340 V), the collisions between the ion-clusters formed during the electrospray process and the nitrogen gas molecules N_2 are so energetic that the ion-clusters can be separated from their molecular environment (molecules of solvent and ligands). In these conditions, the electrospray mass spectrometer acts as an elemental detector. Different mass spectra are obtained according to the lanthanide analysed. They can however be divided into three main classes:

- the lanthanides, which present the ion LnO^+ as a unique form (La, Ce, Pr, Nd, Gd and Tb);
- the lanthanides, which present the ion LnO^+ as a major form (Sm, Dy, Ho, Er, Tm and Lu);
- the lanthanides, which present the ion Ln^+ as a major form (Eu and Yb).

Lanthanum, cerium, praseodymium, neodymium, gadolinium and terbium present as a unique form the bare singly charged lanthanide oxide LnO^+ (where Ln is a lanthanide) (Fig. 3). The presence of singly charged species has been explained by a gas-phase charge reduction reaction occurring during the electrospray process [38].

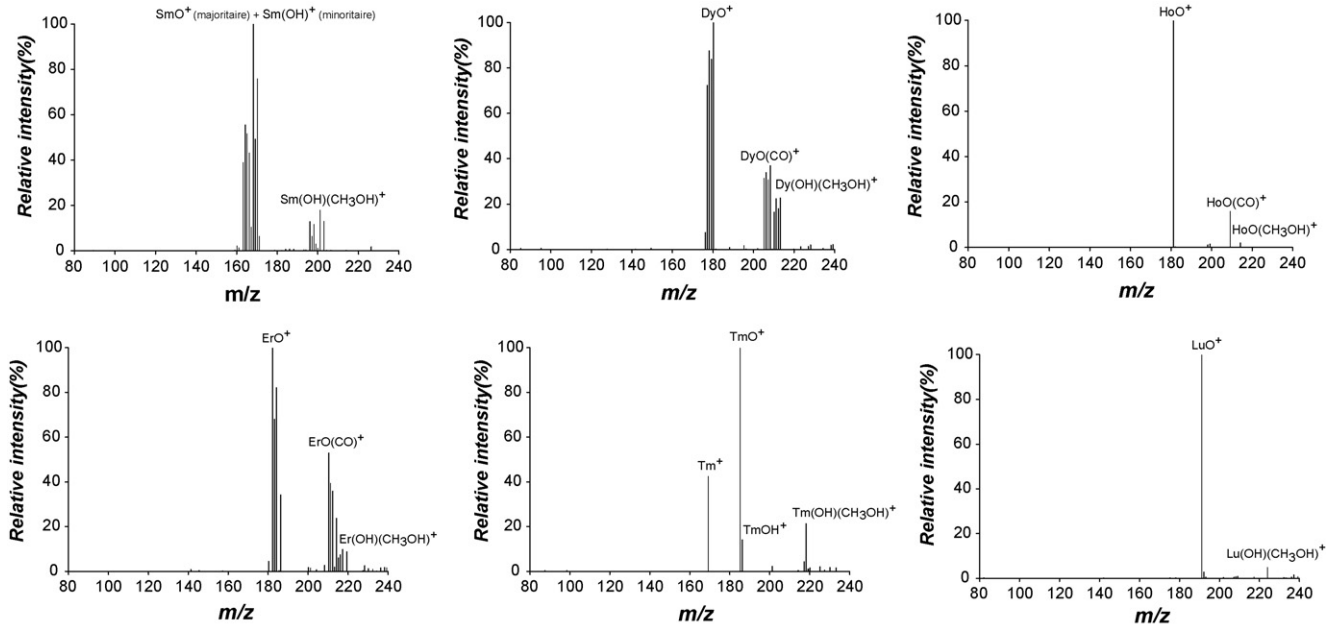

Fig. 4. ESI-MS spectra of the lanthanides, which present the ion LnO^+ as a major form at high fragmentation potentials.

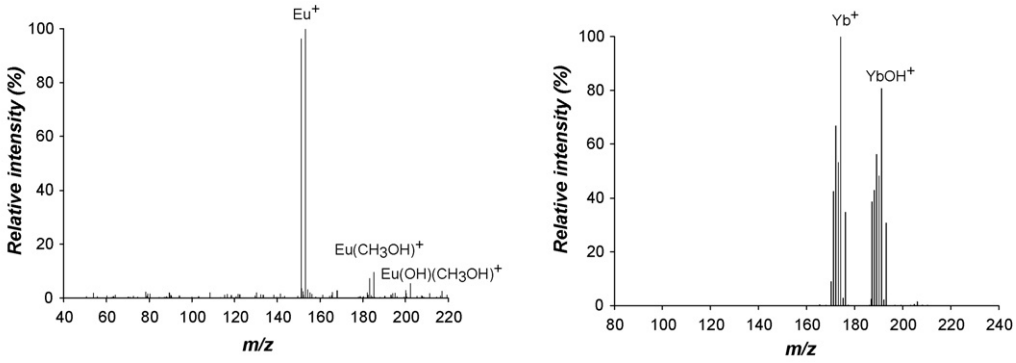

Fig. 5. ESI-MS spectra of the lanthanides, which present the ion Ln^+ as a major form at high fragmentation potentials.

Samarium, dysprosium, holmium, erbium, thulium and lutetium have a slightly different behaviour: the ion LnO^+ is indeed the major form, but some other minor species of the form $LnO(CO)^+$, $LnO(CH_3OH)^+$, $LnOH^+$ and $Ln(OH)(CH_3OH)^+$ may be also present on the mass spectra (Fig. 4). These minor species are related to the major ion LnO^+: the molecular environment (molecules of solvent and ligands) of the ion-clusters formed during the electrospray process is strongly but not totally degraded. Contrary to the other elements of this class, thulium presents the bare singly charged metal ion Tm^+ on its mass spectrum.

Finally, europium and ytterbium have a different behaviour: the bare singly charged metal ion Ln^+ is the major form on their mass spectra (Fig. 5). The minor species $Eu(CH_3OH)^+$ and $Eu(OH)(CH_3OH)^+$ are also present on the europium mass spectrum. A mixture of both Yb^+ and $YbOH^+$ metal ions is observed for ytterbium.

These three main classes can be related to the dissociation energies of the lanthanide oxide bond, as illustrated in Fig. 6A and B [39]. The lanthanides, which present the ion LnO^+ as a unique form (La, Ce, Pr, Nd, Gd and Tb) have a strong dissociation energy ($DE(M^+–O) > 7.67$ eV). The lanthanides, which present the ion LnO^+ as a major form (Sm, Dy, Ho, Er and Lu) have a medium dissociation energy ($5.51\ eV < DE(M^+–O) < 6.29\ eV$). The lanthanides, which present the ion Ln^+ as a major form (Eu and Yb) have a low dissociation energy ($DE(M^+–O) < 4.03$ eV). It is worth to point out that thulium, which presents not only the ion LnO^+ as a major form but also the ion Ln^+ as a minor form on its mass spectrum, has an intermediate dissociation energy between the low and the medium

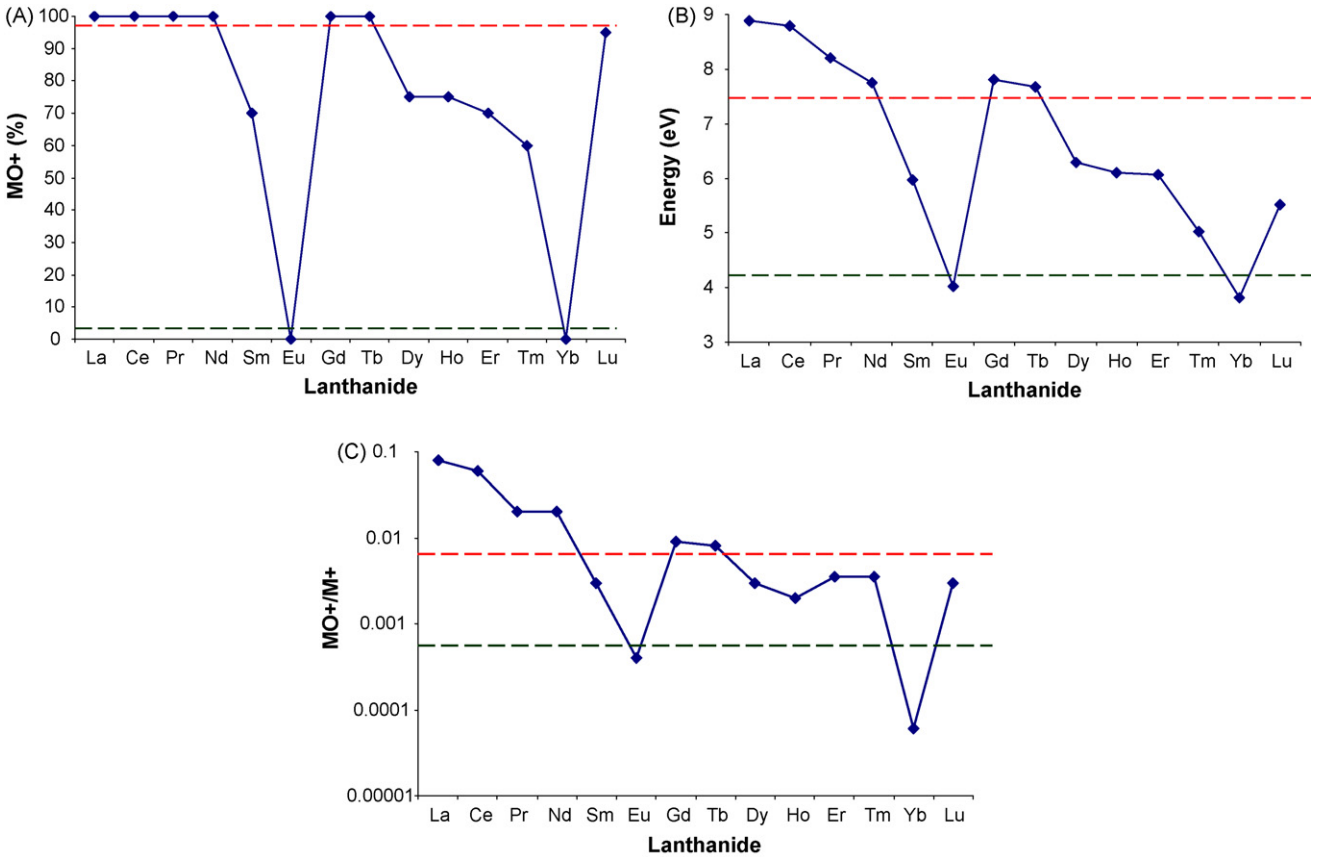

Fig. 6. A: Distribution of lanthanide oxide ions by ESI-MS at high fragmentation potentials. B: Dissociation energies of lanthanide oxide [39]. C: Distribution of lanthanide oxide ions by ICP-MS [40]. The three classes are separated by red and green dashed lines.

dissociation energies (DE_{Tm} = 5.03 eV). Consequently, the lowest the dissociation energy DE(M^+–O) is, the easiest the lanthanide will form the ion Ln^+. These results are in good agreement with those obtained by Stewart and Horlick [19]. It can be also observed that the three classes can be related to the fillings of 4f orbitals, since the dissociation energies of the lanthanide oxides depend directly on the transition energy from the $4f^{n-1}5d6s^2$ electronic state to the $4f^n6s^2$ electronic state [40]. High lanthanide oxide formation for La, Gd and Lu corresponds to an empty 4f orbital for La, a half-filled 4f orbital for Gd and filled 4f orbital for Lu. Low lanthanide oxide formation is observed for Eu and Yb. It is also of interest to observe that the distribution of lanthanide oxide ion by ESI-MS observed at high fragmentation potentials is similar to its distribution for elemental mass spectrometry such as inductively coupled plasma, laser ionisation and spark source ionisation mass spectrometries, the abundance being obviously much lower for these atomic-based spectrometries ($MO^+/M^+ \sim 10^{-4}$–10^{-2}) [41], as illustrated in Fig. 6C. As a consequence, the detection limit achieved by CE–ESI-MS for elemental analysis is much higher than that by CE–ICP-MS. A detection limit in the low μg/mL range has been obtained in this study. This detection limit is comparable to that achieved by direct UV–vis absorption spectrophotometry.

3.6. Low fragmentation potentials

When low fragmentation potentials are applied at the interface (fragmentation potentials lower than 100 V), an ion-solvent cluster distribution is generated during the electrospray process. These ion-clusters are composed of both the metallic species and a "solvation sphere" of solvent molecules, which maintains the metallic species as a stable species in the gas phase at atmospheric pressure. As a result, the ion-cluster distribution should be representative of the species formed in the CE capillary during the electrophoretic separation. The mass spectra observed for the whole lanthanide series as well as the corresponding ion-clusters are presented in Fig. 7 and in Table 2, respectively. Mass spectra, and consequent ion clusters, are quite similar for all lanthanides. The ion-cluster Ln(HIBAO)(picoO)(TRIS)(MeOH)$(H_2O)_6^+$ is predominant for the whole lanthanide series (from *m*/*z* 625.2 for lanthanum to *m*/*z* 661.2 for lutetium). It corresponds to the mixed complex containing HIBA and picolinic acid as ligands surrounded by a "solvation sphere". This mixed complex is expected, since the separation of lanthanides by capillary electrophoresis is achieved by partial complexation using two different ligands (HIBA and picolinic acid). It is likely to be representative of the species formed in the CE capillary during the electrophoretic separation. Other ion-clusters such as Ln(HIBAO)(picoO)$(MeOH)_7(H_2O)^+$ (from *m*/*z* 606.2 for lanthanum to *m*/*z* 633.2 for erbium) correspond also to the mixed complex containing both HIBA and picolinic acid as ligands. Different "solvation spheres" surround the mixed complex: (TRIS)$(MeOH)(H_2O)_6^+$ (*m*/*z* 625.2 for lanthanum) and $(MeOH)_7(H_2O)^+$ (*m*/*z* 606.2 for lanthanum). Since the spray is mainly composed of make-up liquid, it might be expected to have "methanolic solvation spheres". However, some water molecules are coming from the CE capillary, and it has been shown that lanthanides are preferentially solvated by water molecules in water/methanol mixtures [42]. In fact, they are mostly surrounded by water molecules in their inner-sphere. Hydrated clusters may be due either to preferential solvation by water molecules in the condensed phase, to preferential evaporation of methanol, and/or to an exchange of atmospheric water for methanol in the gas phase. It can be also pointed out that in both cases, eight solvent molecules surround the complex; this number ensures probably the stability of the species. Some other low abundant ion-clusters such as Ln(picoO)(MeO)(TRIS)$(MeOH)_5(H_2O)_3^+$ (from *m*/*z* 627.7 for La

Table 2
Mass to charge ratios *m*/*z* and relative abundances observed at low fragmentation potential (100 V) for the different lanthanides

Ion–cluster		La	Ce	Pr	Nd	Sm	Eu	Gd	Tb	Dy	Ho	Er	Tm	Yb	Lu
n(picoO)(MeO)(TRIS)$(MeOH)_5(H_2O)_3^+$	*m*/*z*	627.7 (627.46)	628.7 (628.46)	629.7 (629.46)	630.7 (630.46)	640.7 (640.46)	641.7 (641.47)	646.7 (646.47)	647.7 (647.48)	652.7 (652.48)	653.7 (653.48)	654.7 (654.48)	657.7 (657.48)	662.7 (662.49)	663.7 (663.49)
	%	3	18	14	16	18	23	21	24	22	25	23	57	23	22
Ln(HIBAO)(MeO)(TRIS)$(MeOH)_5(H_2O)_4^+$	*m*/*z*	626.7 (626.47)	627.7 (627.47)	628.7 (628.47)	629.7 (629.47)	639.7 (639.47)	640.7 (640.48)	645.7 (645.48)	646.7 (646.49)	651.7 (651.49)	652.7 (652.49)	653.7 (653.49)	656.7 (656.49)	661.7 (661.50)	662.7 (662.50)
	%	25	21	23	24	26	25	24	28	26	27	25	23	56	62
Ln(HIBAO)(picoO)(TRIS)(MeOH)$(H_2O)_6^+$	*m*/*z*	**625.2** (625.42)	**626.2** (626.42)	**627.2** (627.42)	**628.2** (628.42)	**638.2** (638.42)	**639.2** (639.43)	**644.2** (644.43)	**645.2** (645.44)	**650.2** (650.44)	**651.2** (651.44)	**652.2** (652.44)	**655.2** (655.44)	**660.2** (660.45)	**661.2** (661.45)
	%	**100**	**100**	**100**	**100**	**100**	**100**	**100**	**100**	**100**	**100**	**100**	**100**	**100**	**100**
Ln(HIBAO)(picoO)$(MeOH)_7(H_2O)^+$	*m*/*z*	606.2 (606.42)	607.2 (607.42)	608.2 (608.42)	609.2 (609.42)	619.2 (619.42)	620.2 (620.43)	625.2 (625.43)	626.2 (626.44)	631.2 (631.44)	632.2 (632.44)	633.2 (633.44)	636.2 (636.44)	641.2 (641.45)	642.2 (642.45)
	%	25	28	23	8	24	26	24	38	22	22	9	0	0	0
Ln(picoO)(MeO)$(MeOH)_6(H_2O)^+$	*m*/*z*	502.2 (502.32)	503.2 (503.32)	504.2 (504.32)	505.2 (505.32)	515.2 (515.32)	516.2 (516.33)	521.2 (521.33)	522.2 (522.34)	527.2 (527.34)	528.2 (528.34)	529.2 (529.34)	532.2 (532.34)	537.2 (537.35)	538.2 (538.35)
	%	9	8	13	6	7	14	9	13	17	14	13	8	14	6

The theoretically calculated masses of the different clusters are given between brackets. The predominant species is given in bold. HIBAO: HIBA ligand; picoO: picolinic acid ligand.

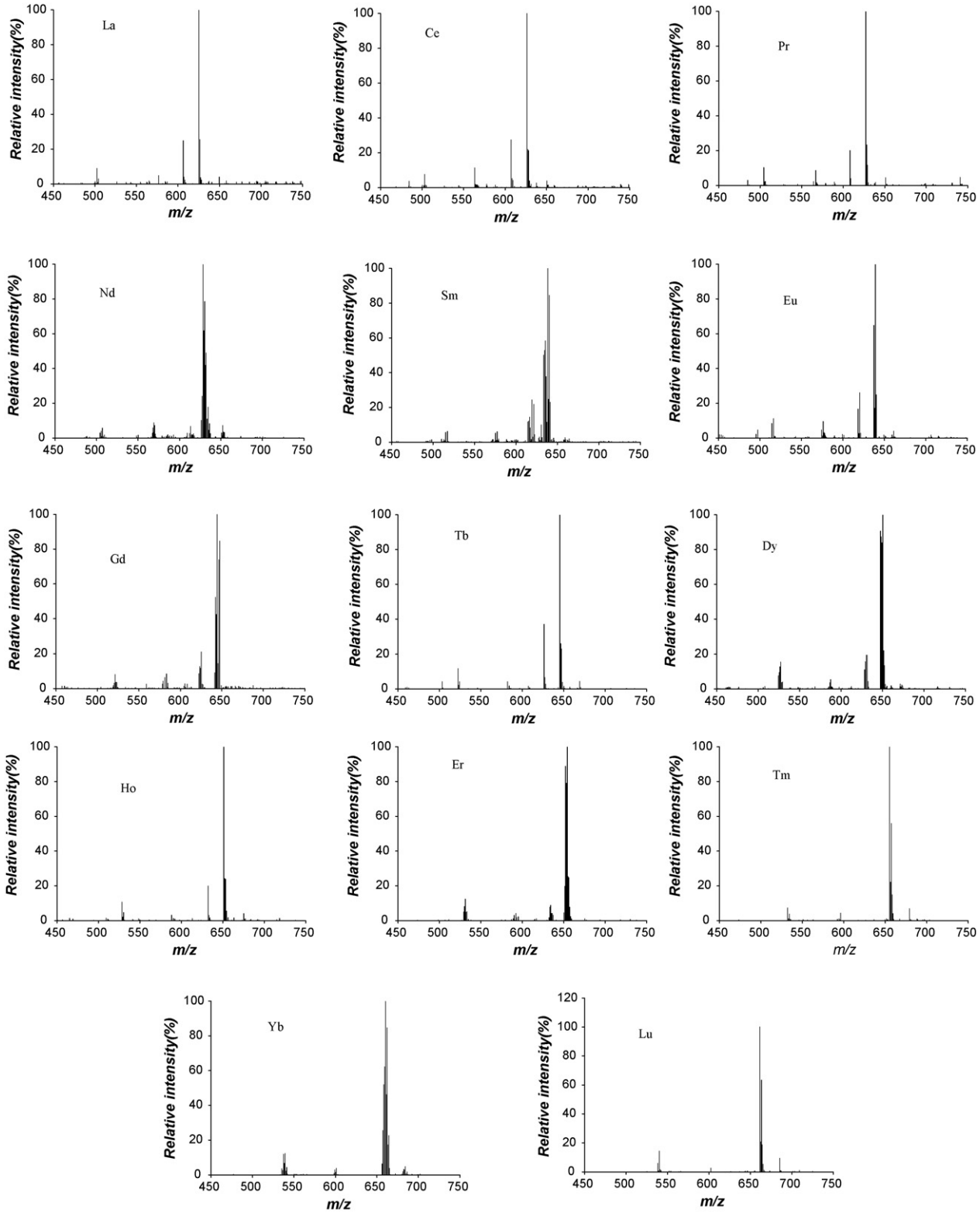

Fig. 7. ESI-MS spectra of the lanthanides at low fragmentation potential (100 V).

to m/z 663.7 for Lu), $Ln(HIBAO)(MeO)(TRIS)(MeOH)_5(H_2O)_4^+$ (from m/z 626.7 for La to m/z 662.7 for Lu) and $Ln(picoO)(MeO)(MeOH)_6(H_2O)^+$ (from m/z 502.2 for La to m/z 538.2 for Lu) correspond to the loss of one ligand. The behaviour of the heaviest lanthanides like thulium, ytterbium and lutetium is different compared to the other lanthanides. The ion-cluster $Ln(HIBAO)(picoO)(MeOH)_7(H_2O)^+$ is not observed for these three elements and higher abundances for other ion-clusters are observed like $Ln(picoO)(MeO)(TRIS)(MeOH)_5(H_2O)_3^+$ m/z 657.7 for thulium, $Ln(HIBAO)(MeO)(TRIS)(MeOH)_5(H_2O)_4^+$ m/z 661.7 and 662.7 for ytterbium and lutetium, respectively. A detection limit in the μg/mL range has been obtained for the use of CE–ESI-MS

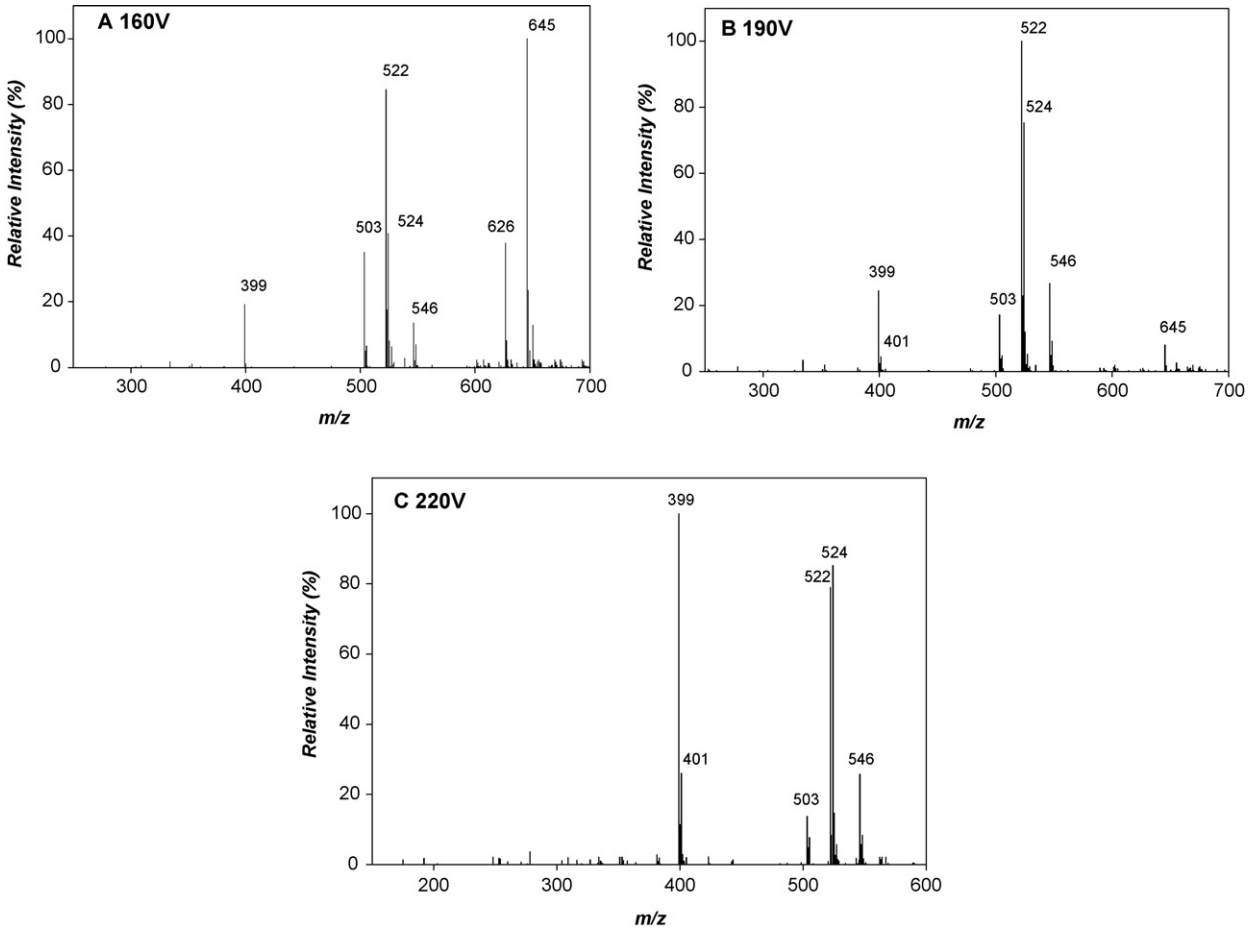

Fig. 8. ESI-MS spectra of terbium Tb at intermediate fragmentation potentials (A: 160 V, B: 190 V and C: 220 V).

as a molecular detector. This detection limit is dependent on the degree of fragmentation of the different clusters, the quantification being based on the predominant ion-cluster.

3.7. Intermediate fragmentation potentials

When intermediate fragmentation potentials are applied at the interface (fragmentation potentials in the range 100–340 V), partial declustering occurs and a wide range of partially declustered species are observed. Mass spectra and corresponding species obtained at three different fragmentation potential values (160 V, 190 V and 220 V) for terbium are presented in Fig. 8 and Table 3, respectively. When increasing the fragmentation potential, a larger number of collisions between the neutral nitrogen curtain gas and analyte ions occurs and declustering is promoted. For a fragmentation potential of 160 V (Fig. 8A), the ion-cluster Tb(HIBAO)(picoO)(TRIS)(MeOH)$(H_2O)_6^+$ (m/z 645.2) observed previously is still predominant. However, some other ion-clusters

Table 3
Mass to charge ratios m/z and relative abundances observed in the intermediary mode (fragmentation potentials: 160 V, 190 V and 220 V) for terbium Tb

	647.7	646.7	645.2	626.2	546.2	524.2	522.2	503.2	401.2	399.2
100 V	24%	28%	**100**%	38%			13%			
160 V	5%	22%	**100**%	39%	16%	41 %	84%	36%		19%
190 V			8%		24%	77%	**100**%	18%		23%
220 V					23%	83%	79%	14%	24%	**100**%

m/z observed	Theoretical value	Corresponding ion-cluster
647.7	647.47	Tb(picoO)(MeO)(TRIS)$(MeOH)_5(H_2O)_3^+$
646.7	646.49	Tb(HIBAO)(MeO)(TRIS)$(MeOH)_5(H_2O)_4^+$
645.2	645.44	**Tb(HIBAO)(picoO)(TRIS)$(MeOH)(H_2O)_6^+$**
626.2	626.44	Tb(HIBAO)(picoO)$(MeOH)_7(H_2O)^+$
546.2	546.32	Tb(HIBAO)(picoO)$(H_2O)_9^+$
524.2	524.30	Tb(HIBAO)(picoO)(MeOH)$(H_2O)_6^+$
522.2	522.34	**Tb(picoO)(MeO)$(MeOH)_6(H_2O)^+$**
503.2	503.33	Tb(HIBAO)(MeO)$(MeOH)_6(H_2O)^+$
401.2	401.19	Tb(HIBAO)(MeO)$(H_2O)_6^+$
399.2	399.23	**Tb$(MeO)_2(MeOH)_5(H_2O)^+$**

The predominant species for each potential is given in bold. HIBAO: HIBA ligand; picoO: picolinic acid ligand.

appear on the mass spectrum. These ion-clusters can be divided into four different classes:

(1) the ion-clusters of the form Tb(HIBAO)(picoO)(solvation sphere)$^+$ such as Tb(HIBAO)(picoO)(TRIS)(MeOH)$(H_2O)_6^+$ (m/z 645.2); Tb(HIBAO)(picoO)$(MeOH)_7(H_2O)^+$ (m/z 626.2) and Tb(HIBAO)(picoO)$(MeOH)(H_2O)_6^+$ (m/z 524.2);
(2) the ion-clusters of the form Tb(picoO)(MeO)(solvation sphere)$^+$ such as Tb(picoO)(MeO)$(MeOH)_6(H_2O)^+$ (m/z 522.2);
(3) the ion-clusters of the form Tb(HIBAO)(MeO)(solvation sphere)$^+$ such as Tb(HIBAO)(MeO)$(MeOH)_6(H_2O)^+$ (m/z 503.2);
(4) the ion-clusters of the form $Tb(MeO)_2$(solvation sphere)$^+$ such as $Tb(MeO)_2(MeOH)_5(H_2O)^+$ (m/z 399.2).

The first class of ion-clusters corresponds to the mixed complex containing picolinic acid and HIBA as ligands surrounded by a "solvation sphere". A loss of TRIS can be observed between the ion-clusters Tb(HIBAO)(picoO)(TRIS)(MeOH)$(H_2O)_6^+$ (m/z 645.2) and Tb(HIBAO)(picoO)(MeOH)$(H_2O)_6^+$ (m/z 524.2) by "Collision-Induced Dissociation" reaction (Eq. (1)).

$$\text{Tb(HIBAO)(picoO)(TRIS)(MeOH)}(H_2O)_6^+(m/z\,645.2) + N_2 \rightarrow \text{Tb(HIBAO)(picoO)(MeOH)}(H_2O)_6^+(m/z\,524.2) + \text{TRIS} + N_2 \quad (1)$$

This loss of TRIS during the electrospray process may be explained by the large size of this molecule compared to the water or methanol molecules.

The second and third classes of ion-clusters correspond to the loss of one ligand (either HIBA or picolinic acid) by the mixed complex followed by a gas-phase charge reduction reaction [26]. Since the ionisation potential of water is higher than that of methanol (11.14 eV and 10.84 eV, respectively), the composition of these ion-clusters will be the following: Tb(picoO)(MeO)(solvation sphere)$^+$ or Tb(HIBAO)(MeO)(solvation sphere)$^+$ [43].

The formation of these two classes can be illustrated by the loss of one ligand from the ion-cluster Tb(HIBAO)(picoO)$(MeOH)_7(H_2O)^+$ (m/z 626.2) (Eqs. (2) and (3)).

$$\text{Tb(HIBAO)(picoO)}(MeOH)_7(H_2O)^+(m/z\,626.2) + N_2 \rightarrow \text{Tb(picoO)(MeO)}(MeOH)_6(H_2O)^+(m/z\,522.2) + \text{HIBAOH} + N_2 \quad (2)$$

$$\text{Tb(HIBAO)(picoO)}(MeOH)_7(H_2O)^+(m/z\,626.2) + N_2 \rightarrow \text{Tb(HIBAO)(MeO)}(MeOH)_6(H_2O)^+(m/z\,503.2) + \text{picoOH} + N_2 \quad (3)$$

The fourth class of ion-clusters corresponds to the loss of the two ligands (both HIBA and picolinic acid) by the mixed complex followed by two gas-phase charge reduction reactions [26]. This class is well represented by the ion-cluster: $Tb(MeO)_2(MeOH)_5(H_2O)^+$ (m/z 399.2) (Eqs. (4) and (5)).

$$\text{Tb(picoO)(MeO)}(MeOH)_6(H_2O)^+(m/z\,522.2) + N_2 \rightarrow Tb(MeO)_2(MeOH)_5(H_2O)^+(m/z\,399.2) + \text{picoOH} + N_2 \quad (4)$$

$$\text{Tb(HIBAO)(MeO)}(MeOH)_6(H_2O)^+(m/z\,503.2) + N_2 \rightarrow Tb(MeO)_2(MeOH)_5(H_2O)^+(m/z\,399.2) + \text{HIBAOH} + N_2 \quad (5)$$

Table 4
Mass to charge ratios m/z and corresponding species observed for the terbium at low fragmentation potential in the presence of ammonia instead of TRIS for buffer pH adjustment

m/z observed	Theoretical value	Corresponding ion-cluster
586.2	586.40	Tb(HIBAO)(picoO)$(MeOH)_3(H_2O)_4(NH_3)_2^+$
567.2	567.39	Tb(HIBAO)(picoO)$(MeOH)_3(H_2O)_2(NH_3)_3^+$
523.2	523.31	**Tb(HIBAO)(picoO)$(MeOH)(H_2O)_5(NH_3)^+$**
463.2	463.29	Tb(HIBAO)$(MeO)(MeOH)_2(H_2O)_4(NH_3)_2^+$
400.2	400.20	Tb(HIBAO) (MeO) $(H_2O)_5(NH_3)^+$

The predominant species is given in bold. HIBAO: HIBA ligand; picoO: picolinic acid ligand.

For a fragmentation potential of 190 V (Fig. 8B), the ion-cluster Tb(picoO)(MeO)$(MeOH)_6(H_2O)^+$ (m/z 522.2) is the predominant one. This ion-cluster has been already observed previously for a fragmentation potential of 160 V, but it was present to a low abundance at this potential. It can be remarked that the ion-cluster Tb(HIBAO)(picoO)(TRIS)(MeOH)$(H_2O)_6^+$ (m/z 645.2), which was the major species at 100 V and 160 V, is present to a low abundance at 190 V.

When increasing the fragmentation potential at 220 V (Fig. 8C), the predominant ion-cluster becomes $Tb(MeO)_2(MeOH)_5(H_2O)^+$ (m/z 399.2). It corresponds to the loss of picolinic acid from the ion-cluster Tb(picoO)(MeO)$(MeOH)_6(H_2O)^+$ (m/z 522.2), which was predominant at 190 V. Ion-clusters of the form Tb(HIBAO)(picoO)(solvation sphere)$^+$ are no more observed at 220 V.

For fragmentation potentials higher than 220 V, the predominant species becomes the bare singly charged terbium oxide TbO^+ (m/z 175.2).

Thus, the intermediate fragmentation potentials enable the study of the different steps of declustering.

3.8. Influence of the buffer composition

Formic acid has no role in the process of partial complexation involved in the lanthanide separation, but it modifies the medium conductivity in order to increase the separation. Formic acid has been eliminated from the CE buffer composition to study its influence on the ion-clusters observed for the different fragmentation potentials. The mass spectra obtained using for the capillary electrophoretic separation a buffer without formic acid resulted the same as those obtained when formic acid is a constituent of the CE buffer. This result confirms that no ion-cluster containing formic acid molecules in its "solvation sphere" is formed, as it has been previously observed.

3.8.1. Influence of the presence of ammonia instead of TRIS for buffer pH adjustment

TRIS is usually used in the separation buffer for pH adjustment in order to have a low capillary electrophoresis current thus reducing Joule effect during the electrophoretic separation. TRIS molecules have been observed in the "solvation sphere" of ion-clusters at low fragmentation potentials. To study the influence of the chemical used for buffer pH adjustment on the m/z ratios and consequent ion-clusters, TRIS has been replaced by ammonia. When high fragmentation potentials are applied, similar mass spectra are obtained with only the singly charged bare lanthanide oxide present. On the contrary, when low fragmentation potentials are applied, m/z ratios and consequent ion-clusters are different (Table 4). The predominant ion-cluster, observed at m/z 523.2, can be attributed to Tb(HIBAO)(picoO)$(MeOH)(H_2O)_5(NH_3)^+$. This ion-cluster corresponds to the mixed complex containing picolinic acid and HIBA as ligands surrounded by the "solvation sphere":

$(MeOH)(H_2O)_5(NH_3)^+$. This "solvation sphere" is very similar to that obtained when using TRIS: $(MeOH)(H_2O)_6$. A molecule of ammonia has just replaced a molecule of water in the "solvation sphere". The ion-cluster Tb(HIBAO)(picoO)(MeOH)$(H_2O)_6^+$ (m/z 524.2) is also present to a low abundance when using ammonia, showing an exchange between a molecule of water and a molecule of ammonia in the "solvation sphere" during the electrospray process (Eq. (7)).

$$\mathrm{Tb(HIBAO)(picoO)(MeOH)(H_2O)_6^+}\,(m/z\,524.2) + \mathrm{NH_4^+} \rightarrow \mathrm{Tb(HIBAO)(picoO)(MeOH)(H_2O)_5(NH_3)^+}\,(m/z\,523.2) + \mathrm{H_3O^+} \quad (7)$$

The ion-cluster Tb(HIBAO)(MeO)$(H_2O)_5(NH_3)^+$ (m/z 400.2) corresponding to the loss of the ligand picolinic acid by the major ion-cluster Tb(HIBAO)(picoO)(MeOH)$(H_2O)_5(NH_3)^+$ (m/z 523.2) is also present on this mass spectrum (Eq. (8)).

$$\mathrm{Tb(HIBAO)(picoO)(MeOH)(H_2O)_5(NH_3)^+}\,(m/z\,523.2) + \mathrm{N_2} \rightarrow \mathrm{Tb(HIBAO)(MeO)(H_2O)_5(NH_3)^+}\,(m/z\,400.2) + \mathrm{picoOH} + \mathrm{N_2} \quad (8)$$

Other low abundant ion-clusters present molecules of ammonia in their "solvation spheres". This indicates that ammonia can be easily included in the "solvation spheres" during the electrospray process due to probably some of its physico-chemical properties as size and polarisability, which are comparable to those of water or methanol molecules.

4. Conclusion

The multi-component elemental and molecular analysis of the whole lanthanide series has been performed by coupled capillary electrophoresis-electrospray mass spectrometry. Lanthanide isobaric interferences have been overcome by using a previous chemical separation before mass spectrometric analysis. The three ESI-MS modes have been described in terms of fragmentation potentials. For a high fragmentation potential, the system operates as an elemental detector and in the spectra mainly singly charged lanthanide oxide or lanthanide metal ion are observed. These results correlate with the lanthanide oxide bond dissociation energies and with the lanthanide electronic properties. The distribution of lanthanide oxide ions by ESI-MS in this mode is comparable to its distribution in inductively coupled plasma, laser ionisation and spark source ionisation mass spectrometry. For a low fragmentation potential, the system operates as a molecular detector and structural information on the mixed complex formed in the CE capillary during the electrophoretic separation can be obtained. The distribution and relative abundance depend on the solution properties and the fragmentation potential applied. The intermediate fragmentation potentials enable the study of the different steps of declustering.

References

[1] V.L. Dressler, D. Pozebon, A. Matusch, J.S. Becker, Int. J. Mass Spectrom. 266 (2007) 25.
[2] J.G. Sen Gupta, Talanta 31 (1984) 1045.
[3] M. Ochsenkühn-Petropulu, T. Lyberopulu, G. Parissakis, Anal. Chim. Acta 296 (1994) 305.
[4] M.I. Rucandio, Anal. Chim. Acta 264 (1992) 333.
[5] W.R. Pedreira, C.A. da Silva Queiroz, A. Abrao, M.M. Pimentel, J. Alloys Compd. 374 (2004) 129.
[6] N.M. Raut, L. Huang, S.K. Aggarwal, K. Lin, Spectrochim. Acta B 58 (2003) 809.
[7] W.R. Pedreira, J.E.S. Sarkis, C.A. da Silva Queiroz, C. Rodrigues, I.A. Tomiyoshi, A. Abrao, J. Solid State Chem. 171 (2003) 3.
[8] M. He, B. Hu, Z. Jiang, Anal. Chim. Acta 530 (2005) 105.
[9] S. Augagneur, B. Medina, J. Szpunar, R. Lobinski, J. Anal. At. Spectrom. 11 (1996) 713.
[10] K.E. Jarvis, J. Anal. At. Spectrom. 4 (1989) 563.
[11] F.E. Lichte, A.L. Meier, J.G. Crock, Anal. Chem. 59 (1987) 1150.
[12] T. Uchino, M. Ebihara, N. Furuta, J. Anal. At. Spectrom. 10 (1995) 25.
[13] T. Hirata, H. Shimizu, T. Akagi, H. Sawatari, A. Masuda, Anal. Sci. 4 (1988) 637.
[14] A.R. Date, D. Hutchinson, J. Anal. At. Spectrom. 2 (1987) 269.
[15] B. Casetta, A. Giaretta, G. Mezzacasa, At. Spectrosc. 11 (1990) 222.
[16] D.S. Braverman, J. Anal. At. Spectrom. 7 (1992) 43.
[17] G.R. Agnes, G. Horlick, Appl. Spectrosc. 48 (1994) 655.
[18] G.R. Agnes, G. Horlick, Appl. Spectrosc. 46 (1992) 401.
[19] I. Stewart, G. Horlick, Anal. Chem. 66 (1994) 3983.
[20] A.T. Blades, P. Jayaweera, M.G. Ikonomou, P. Kebarle, Int. J. Mass Spectrom. 101 (1990) 325.
[21] A.T. Blades, P. Jayaweera, M.G. Ikonomou, P. Kebarle, Int. J. Mass Spectrom. 102 (1990) 251.
[22] J.W. Olesik, K.K. Thaxton, S.V. Olesik, J. Anal. At. Spectrom. 12 (1997) 507.
[23] C. Moulin, N. Charron, G. Plancque, H. Virelizier, Appl. Spectrosc. 6 (2000) 54.
[24] C. Moulin, B. Amekraz, S. Hubert, V. Moulin, Anal. Chim. Acta 441 (2001) 269.
[25] F. Allain, H. Virelizier, C. Moulin, C. Jankowski, J.F. Dozol, J.C. Tabet, Spectroscopy 14 (2000) 127.
[26] C. Lamouroux, C. Moulin, J.C. Tabet, C. Jankowski, Rapid Commun. Mass Spectrom. 14 (2000) 1869.
[27] C. Moulin, B. Amekraz, S. Colette, D. Doizi, C. Jacopin, C. Lamouroux, G. Plancque, J. Alloys Compd. 408–412 (2006) 1242.
[28] S. Colette, B. Amekraz, C. Madic, L. Berthon, G. Cote, C. Moulin, Inorg. Chem. 42 (2003) 2215.
[29] S. Colette, B. Amekraz, C. Madic, L. Berthon, G. Cote, C. Moulin, Inorg. Chem. 41 (2002) 7031.
[30] J.J. Corr, J.F. Anacleto, Anal. Chem. 68 (1996) 2155.
[31] O. Schramel, B. Michalke, A. Kettrup, J. Chromatogr. A 819 (1998) 231.
[32] L. Perna, F. Bocci, L. Aldave de las Heras, J. de Pablo, M. Betti, J. Anal. At. Spectrom. 17 (2002) 1166.
[33] A. Pitois, L. Aldave de las Heras, M. Betti, Int. J. Mass Spectrom. 270 (2008) 118.
[34] J.A. Day, J.A. Caruso, J.S. Becker, H.-J. Dietze, J. Anal. At. Spectrom. 15 (2000) 1343.
[35] N. Öztekin, F.B. Erim, J. Chromatogr. A 924 (2001) 541.
[36] G.J. Van Berkel, F. Zhou, Anal. Chem. 67 (1995) 2916.
[37] J.A. Caruso, K.L. Sutton, K.L. Ackley, Elemental Speciation New Approaches for Trace Element Analysis, 33, Elsevier, 2000.
[38] P. Kebarle, L. Tang, Anal. Chem. 65 (1993) 972A.
[39] E. Murad, D.L. Hildebrand, J. Chem. Phys. 73 (1980) 4005.
[40] J.S. Becker, H.-J. Dietze, J. Anal. Atom. Spectrom. 10 (1995) 637.
[41] J.S. Becker, G. Seifert, A. Saprykin, H.-J. Dietze, J. Anal. Atom. Spectrom. 11 (1996) 643.
[42] F. Tanaka, Y. Kawasaki, S. Yamashita, J. Chem. Soc. 84 (1988) 1083.
[43] D. Lide (Ed.), CRC Handbook of Chemistry and Physics, 79th ed., CRC Press, Boca Raton/Boston/London/New York/Washington, DC, 1998.